processes

MDPI

Article

Fire Characteristics and Water Mist Cooling Measures in the Coal Transportation Process of a Heavy-Haul Railway Tunnel in Shanxi Province

Wenjin He [1], Maohai Fu [2,*], Lv Xiong [1] and Shiqi Zheng [3]

[1] Institute of Rail Transit, Guangdong Communication Polytechnic, Guangzhou 510650, China; hewenjean@gdcp.edu.cn (W.H.); gdcprailh@163.com (L.X.)
[2] School of Mechanical Engineering, Southwest Jiaotong University, Chengdu 610095, China
[3] Guangzhou Municipal Engineering Design & Research Institute Co., Ltd., Guangzhou 510000, China; zhengsq@gzmedri.com
* Correspondence: gd3987@outlook.com

Abstract: This study investigates the spread patterns of tunnel fires and examines issues related to emergency response. It focuses on the temperature characteristics, spread patterns, conditions leading to multi-source fires, and the efficacy of water mist suppression methods in heavy-haul railway tunnel fires. The research employs theoretical derivations and numerical simulations to achieve its objectives. It was discovered that, during a fire in a heavy-haul railway tunnel, the temperature inside the tunnel can exceed 500 °C. Furthermore, depending on the nature of the goods transported by the train and under specific wind speed conditions, the fire source has the potential to spread to other carriages, resulting in a multi-source fire. Using the numerical simulation software Pyrosim 2022, various wind speed conditions were simulated. The results revealed that at lower wind speeds, the smoke demonstrates a reverse flow phenomenon. Concurrently, when the adjacent carriage on the leeward side of the fire is ignited, the high-temperature reverse flow smoke, along with the thermal radiation from the flames, ignites combustible materials in the adjacent carriage on the windward side of the burning carriage. Through theoretical derivation and numerical simulation, the critical wind speed for the working conditions was determined to be 2.14 m/s. It was found that while a higher wind speed can lead to a decrease in temperature, it also increases the flame deflection angle. When the wind speed exceeds 2.4 m/s, although the temperature significantly drops in a short period, the proximity of combustible materials on the leeward side of the carriage becomes a concern. At this wind speed, the flame deflection angle causes heat radiation on the leeward side, specifically between 0.5 m and 3 m, to ignite the combustible materials on the carriage surface, resulting in fire spread and multiple fire incidents. The relationship between wind speed and the angle of deflection from the fire source was determined using relevant physics principles. Additionally, the relationship between wind speed and the trajectory of water mist spraying was established. It was proposed to optimize the position of the water mist based on its deviation, and the results indicated that under critical wind speed conditions, when the water mist spraying is offset approximately 5 m towards the upwind side of the fire source, it can act more directly on the surface of the fire source. Numerical simulation results show a significant reduction in the maximum temperature and effective control of fire spread. Under critical wind speed conditions, the localized average temperature of the fire decreased by approximately 140 °C when spraying was applied, compared to the conditions without spraying, and the peak temperature decreased by about 190 °C. This modification scheme can effectively suppress the threat of fire to personnel evacuation under simulated working conditions, reflecting effective control over

check for updates

Academic Editors: Feng Du, Leilei Si, Chaojun Fan and Qiming Zhuo

Received: 22 April 2025
Revised: 26 May 2025
Accepted: 29 May 2025
Published: 5 June 2025

Citation: He, W.; Fu, M.; Xiong, L.; Zheng, S. Fire Characteristics and Water Mist Cooling Measures in the Coal Transportation Process of a Heavy-Haul Railway Tunnel in Shanxi Province. *Processes* **2025**, *13*, 1789. https://doi.org/10.3390/pr13061789

Copyright: © 2025 by the authors. Licensee MDPI, Basel, Switzerland. This article is an open access article distributed under the terms and conditions of the Creative Commons Attribution (CC BY) license (https://creativecommons.org/licenses/by/4.0/).

fires. Additionally, it provides theoretical support for the study of fire patterns in tunnels and emergency response measures.

Keywords: tunnel fires; numerical simulation; multiple ignition sources; flame deflection angle; water mist optimization

1. Introductory

Heavy-duty railroads have garnered significant attention in the realm of freight transportation due to their characteristics of large capacity, high efficiency, and low cost. The advantages of heavy-duty railroad transportation are more pronounced compared to other modes of transportation, leading to rapid development in resource-rich countries such as the United States, China, Canada, and Australia. Heavy-duty railroad transportation is particularly common for goods such as coal and ore, which present risks of spontaneous combustion and flammability. As heavy-duty railroads expand their networks extensively, the number of tunnel sections has also increased. Due to the long transportation distances associated with heavy railroads, the conditions within tunnels differ significantly from those of other passenger tunnels [1]. The relatively enclosed environment of tunnels, which contains a substantial amount of electrical equipment, poses unique risks. When heavy trains carrying flammable products traverse these tunnels, they can distribute a considerable quantity of combustible and flammable materials throughout the space. This specific environment increases the likelihood of fire incidents, with the potential hazards being significantly greater than in other heavily loaded sections. Additionally, the number of fire-causing factors within the tunnel is notably elevated, including incidents such as train collisions, electrical fires, and the friction of trains igniting combustible materials [2]. In 2001, a fire was triggered in the St. Gotthard tunnel in Switzerland due to the impact of goods falling off the walls. Additionally, the properties of the cargo can increase the incidence of fire; for instance, coal, which is a primary transport cargo for heavy trains, may accelerate the oxidation process under certain environmental conditions. When heavy trains pass through rail tunnels, the heat generated can accumulate, leading to the spontaneous combustion of coal piles [3–6]. This phenomenon has been observed in the Daqin Railway in China, where a fire was ignited by the spontaneous combustion of coal during transport. When a fire occurs in a tunnel, the unique characteristics of its internal structure can cause temperatures to exceed 1000 °C. The smoke generated by such fires is difficult to eliminate, leading not only to potential casualties but also to significant damage to the tunnel structure due to the extreme heat. Therefore, studying the characteristics of fires in heavy railroad tunnels and implementing relevant measures to control both the fire and the internal temperature can effectively mitigate the impacts of such incidents on both individuals and the environment [7]. This research is crucial for enhancing the overall safety of heavy railroad tunnels.

Scholars from around the globe have extensively studied tunnel fires, primarily through fire experiments, numerical simulations, and other methodologies to enhance the theoretical understanding of tunnel fires. Jae Seong Roh, Seung Shin Yang, et al. [8] utilized scaled-down model fire experiments to examine the heat release rate from fires in various ventilation environments, establishing a positive correlation between wind speed and heat release rate under specific conditions. E. Blanchard, P. Boulet, et al. [9] conducted 4 MW oil pan fire experiments using a tunnel model to investigate heat loss during each phase of the fire, confirming that wind speed is positively correlated with the heat release rate. Furthermore, they analyzed the heat loss associated with each stage of their fire experiments and

validated their findings through numerical simulations. McGrattani et al. [10] employed the numerical simulation software FDS to replicate a tanker truck fire in the Howard Street Tunnel. Their findings indicated that the temperature on the surface of the fire source exceeded 1000 °C, while temperatures in the vicinity of the fire source reached over 500 °C. Similarly, Ciro Caliendo, Paolo Ciambelli [11], and colleagues utilized numerical simulation software to examine the temperature distribution within a bi-directional highway tunnel during a vehicle fire. Their results revealed that an increase in the number of fire sources correlates with a heightened risk within the tunnel [12–14]. In heavy railroad tunnel fires, the presence of a significant amount of flammable materials carried by trains makes the study of the temperature field under various boundary conditions particularly crucial. Tunnels tend to accumulate heat and are susceptible to conditions such as ventilation, which can lead to the ignition of unignited combustible materials present in the train, resulting in multiple fire sources. Among the factors influencing temperature distribution, wind speed in the tunnel is one of the most critical. Delichatsios [15] investigated the temperature distribution characteristics of promenade fires in naturally ventilated environments and described the temperature decay equation. Thomas [16,17] analyzed the smoke backward recession phenomenon caused by wind speed in tunnels, examining inertial and buoyancy forces to derive a dimensionless empirical equation for the backward recession length of high-temperature smoke. Hu longhua [18,19] conducted full-scale fire experiments to investigate smoke propagation from the tunnel roof and developed a fire exponential decay model by integrating momentum equations. Additionally, Wu and Bakar [20] performed fire experiments in tunnels with various cross-section shapes, identifying the critical wind speed for their fires and establishing a dimensionless critical wind speed model.

In heavy railroad tunnel fires, the unique characteristics of the goods transported by trains necessitate careful consideration of wind speed. Insufficient wind speed can lead to smoke backflow and may cause flames to be drawn towards the upwind side, exacerbating the fire's spread. Conversely, excessively high wind speeds can reduce the peak temperature within the tunnel [21]. However, they can also alter the flame's trajectory, causing it to deflect excessively downwind. This deflection can result in heat radiation igniting flammable materials in the downwind carriages, further contributing to fire proliferation. Therefore, studying fires in heavy railroad tunnels is of paramount importance. Utilizing numerical simulation software to analyze the impact of wind speed on flame behavior and temperature distribution is essential for enhancing fire prevention and emergency response capabilities in these environments.

2. Numerical Simulation Modeling

2.1. Introduction to Pyrosim Numerical Simulation Software

Pyrosim numerical simulation software, developed by Thunderhead Engineering in the United States, employs computational fluid dynamics methods to simulate flame combustion, heat transfer, and smoke movement in designed scenarios during fire events. It primarily focuses on low-Mach fluid flow and utilizes the mixed fraction method for combustion modeling. The software predominantly implements large eddy simulation and direct numerical simulation techniques for turbulence simulation.

Pyrosim is solved using the Fire Dynamics Simulator (FDS) solver, which is governed by several key equations: the mass conservation equation, the momentum conservation equation, the energy conservation equation, the component transport equation, and the equation of state [22,23]. The mass conservation equation is articulated in Equation (1).

$$\frac{\partial \rho}{\partial t} + \nabla \cdot (\rho u) = 0 \tag{1}$$

where ρ represents the gas density, kg/m^3; t denotes time, s; u is the velocity vector, m/s; and ∇ is the dispersion operator, 1/m. The momentum conservation equation is presented in Equation (2).

$$\frac{\partial u}{\partial t} = \vec{F} - \frac{1}{\rho}\nabla p + v\nabla^2 u - (u \cdot \nabla)u \quad (2)$$

where $\vec{F}$ is the vector of external force acting on the fluid, N/m^3; v is the coefficient of kinematic viscosity. The energy conservation equation is shown in Equation (3).

$$\frac{\partial(\rho h)}{\partial t} + \nabla \cdot (\rho h u) = \frac{\mathrm{D}p}{\mathrm{D}t} + \nabla \cdot (k\nabla T) + q''' - q''_{rad} + q_{chem} \quad (3)$$

where h is the specific enthalpy, J/kg; T is the temperature, K; k is the thermal conductivity, W/(m·k); q''' is the volumetric heat source, W/m^3; q'' is the radiative heat loss, W/m^3; q_{chem} is the chemical reaction exothermic rate, W/m^3. The component transportation equation is Equation (4).

$$\frac{\partial(\rho Z)}{\partial t} + \nabla \cdot (\rho Z u) = \nabla \cdot (\rho D \nabla Z) \quad (4)$$

where Z is the mixing fraction; D is the diffusion coefficient, m^2/s.

At the same time, Pyrosim provides the Smokeview function, which is able to visualize the changes in smoke flow in a fire scenario.

2.2. Fire Full-Scale Modeling

To align the research conditions more closely with the actual project, a heavy-duty railroad transportation tunnel in Shanxi was selected for research visits and investigations. This study is conducted in accordance with the International Union of Railways standard UIC564-2 (International Union of Railways, 2019) [24]. A 500 m long tunnel with a rectangular cross-section measuring 4.8 m in width and 5.5 m in height was established. The wall thickness is 0.2 m, taking into account the wall material used in the actual project. This setup aims to facilitate a more thorough investigation of temperature field variations.

Considering the wall material used in the actual project and to facilitate a more effective study of the temperature field changes, the wall material is selected to be adiabatic. Within the tunnel, a transport carriage is established; this carriage is an open car designed for coal transport. The dimensions of the carriage are as follows: length of 13.5 m, width of 3 m, and height of 2 m. Additionally, several carriages are established with an interval of 0.5 m between them. The coal within the carriage is leveled with the upper end of the compartments. The primary parameters are summarized in Table 1.

Table 1. Geometric parameters and boundary conditions of carriages.

Setting Elements	Parameters
Transport	Coal
Thickness of sidewalls of carriages	3 mm
Thickness of the underside of the carriages	5 mm
Carriage end wall thickness	4 mm
Diameter of carriage wheels	920 mm
Carriage material	Steel

In the fire source, the spontaneous combustion of the coal pile is simulated, with the starting source chosen as the t^2 fire model. This model primarily simulates the combustion process of coal's spontaneous combustion, with the initial combustion point located at the top of the coal in the wagon. The fire model can be expressed as $Q = at^2$, where Q represents the heat release rate measured in kilowatts, kW; while a is the fire growth coefficient in kW/s^2; and t is the time required for the fire to achieve its maximum heat release rate, s.

Based on the combustion characteristics of coal, the fire power in heavy railroad tunnels typically ranges from 5 to 30 MW. Additionally, spontaneous combustion fires in coal piles usually exhibit fire growth coefficients between 0.011 and 0.044. For the purposes of this analysis, Q is established at 10,000 kW, t is set at 300 s, and the fire growth coefficient a is defined as 0.011 kW/s^2. Simultaneously, the coal in the compartment undergoes a pyrolysis reaction. The ignition point of coal typically exceeds 300 °C; therefore, once the temperature of the coal reaches 300 °C, it can ignite. The heat release rate during coal combustion is set at 1000 kW/m^2, achieving its maximum heat release rate after 300 s of combustion. The geometric model diagram of the fire scene is illustrated in Figure 1.

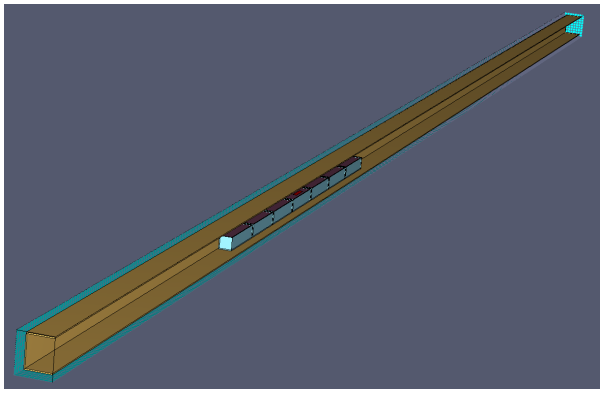


Figure 1. Model diagram of tunnel fire.

Figure 1 illustrates that the central train carriages are designated as the fire carriages. To study the temporal changes in temperature, CO concentration, and other fire characteristics, the center of the fire source in the tunnel serves as a reference point. Thermocouples, smoke concentration sensors, CO concentration sensors, and pressure sensors are installed at vertical heights of 5.5 m, positioned at intervals of 5 m on both the anterior and posterior sides of the fire source. In order to study the fire dynamics at the top of the coal pile within the compartments under varying wind conditions, we examined the temperature field changes at a vertical height of 3.92 m. Utilizing a consistent sensor layout and type, we positioned thermocouples and CO concentration sensors at a height of 1.6 m, which corresponds to the average height of a human eye. These sensors were strategically placed 0.3 m from the walls on both the left and right sides of the carriage. Additionally, we established the fire's center point and deployed monitoring points every 5 m both in front of and behind the carriage. The primary objective of this study is to analyze the escape environment during a fire and to improve rescue operations. The arrangement of the monitoring points is illustrated in Figures 2 and 3.

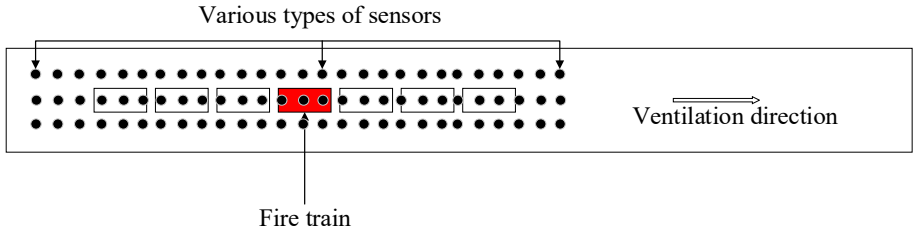


Figure 2. Horizontal arrangement of various types of sensors in the fire tunnel.

In the figure, the black filled circles represent various types of sensors, while the red rectangle indicates the carriage where the initial fire originated. The direction of the arrow illustrates the wind direction, which was analyzed in the simulation by varying wind speeds to observe changes in the temperature field.

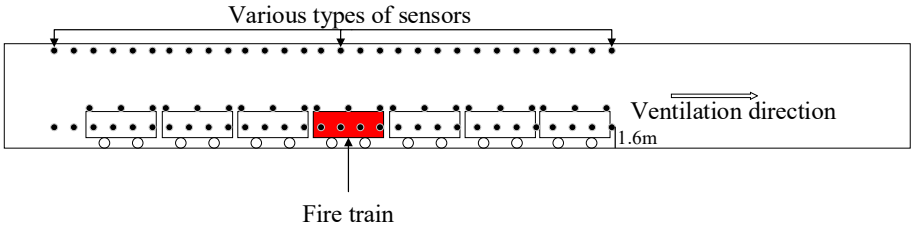


Figure 3. Vertical arrangement of various types of sensors in the fire tunnel.

2.3. Mesh Partitioning and Mesh Irrelevance Test

In Pyrosim, the grid division of the fire model significantly affects the accuracy of fire simulations. Generally, smaller grid sizes lead to more accurate computational results; however, they also increase the computation time required by the computer. Research presented in paper [25] compares temperature trends under various grid size conditions. This analysis is further contextualized by the grid size division standards provided in the FDS user manual, which can be expressed by Equation (5).

$$D^* = \left(\frac{Q}{\rho_0 c_P T_0 \sqrt{g}}\right)^{\frac{2}{5}} \tag{5}$$

where D^* is the characteristic diameter of the fire source, m; ρ_0 is the density of ambient air, kg/m^3; c_p is the specific heat capacity of air, which takes the value of kJ/(kg·K); T_0 is the temperature, K; and g is the acceleration of gravity, m/s^2. The characteristic diameter of the fire source can be calculated to be about 2.34 m, and the results of the calculations are relatively accurate when the characteristic diameter of the fire source is 1/4 to 1/16 times the size of the mesh. Therefore, in order to ensure the accuracy of the fire simulation results, the grid-independence test is carried out for the fire simulation.

The temperature trend directly above the fire source for mesh sizes ranging from 0.15 m to 0.5 m is illustrated in Figure 4. It can be observed that the temperature trends across the four grid sizes are consistent, with values remaining largely similar. The maximum error observed does not exceed 15 °C. Therefore, for mesh sizes of 0.15 m, 0.3 m, 0.4 m, and 0.5 m, the fire simulation results are deemed accurate. However, it is important to note that the mesh size significantly affects the simulation time on the computer. To ensure relative accuracy, a mesh size of 0.3 m was found to yield results most similar to those obtained with a mesh size of 0.15 m while also providing relatively high computational efficiency, utilizing a total of 1,066,250 meshs.

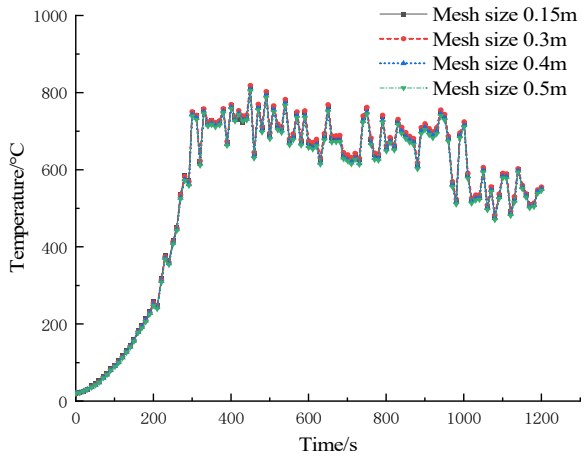


Figure 4. Mesh size 0.15 m, 0.3 m, 0.4 m, 0.5 m temperature comparison chart of the same measurement point.

3. Study on the Fire Characteristics of Heavy Railway Tunnels

3.1. Study on the Fire Spreading Characteristics of Heavy Railroad Trains

In the simulation of coal pile fire within a heavy railroad tunnel train under ventilation conditions of 0 m/s and 1 m/s, it was observed that the combustion behavior and temperature distribution of the fire conformed to general principles in the absence of wind. When a fire occurs, high-temperature smoke impacts the roof, spreading uniformly along the roof walls and forming a roof jet. Given that coal is the primary cargo transported by the train, a low roof height hampers the efficient expulsion of high-temperature smoke, leading to the accumulation of local hotspots. Consequently, the temperature above the train remains elevated, potentially igniting other transport vehicles that are not on fire, thus facilitating a broader spread of the fire. Since the train primarily transports coal, inadequate roof height further delays the timely expulsion of smoke, exacerbating local heat buildup. This causes the temperature above the train to rise significantly, which may lead to the ignition of other coal in the transportation vehicles without an open flame, thereby facilitating the spread of fire and the occurrence of multiple flames. Figure 5 illustrates the fire occurring at different moments, represented by a temperature cloud diagram.

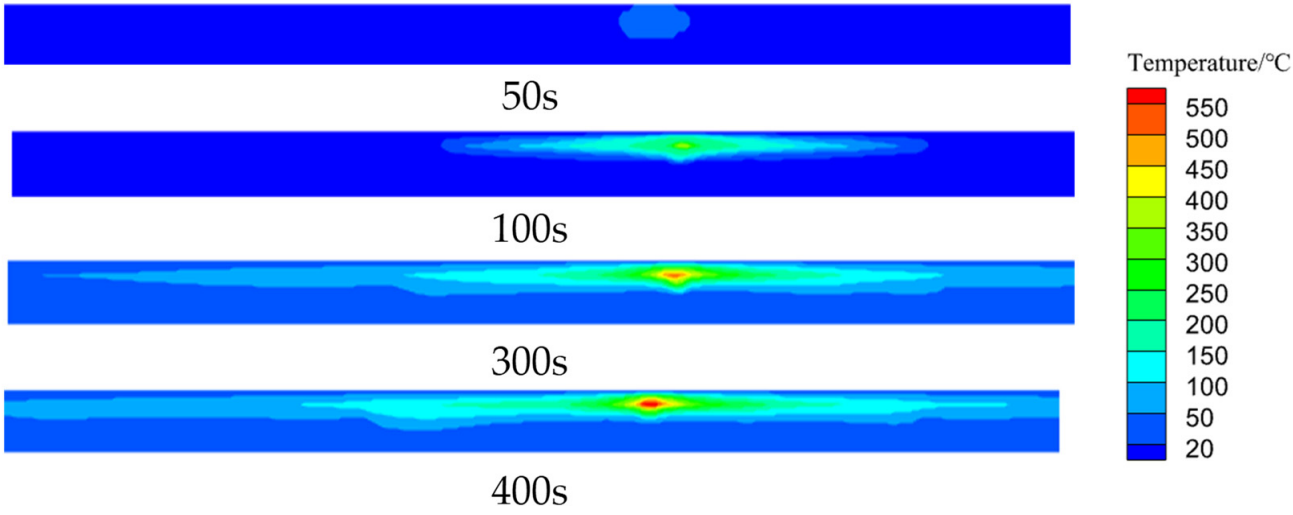


Figure 5. Temperature cloud of horizontal cross-section in the tunnel at different moments.

As illustrated in Figure 5, under windless conditions, when the heat release rate of a single fire source reaches its peak, the temperature of the ceiling is notably elevated, reaching 550 °C. The vertical height is 3.9 m, at which the exposed surface of the coal transported in the carriage has reached a temperature of 230 °C. Given that the general ignition point of coal is approximately 300 °C, the temperature has not yet reached this critical threshold. Consequently, the risk of fire spreading to adjacent carriages remains relatively low. The temperature did not reach the ignition point of the coal, resulting in a relatively low risk of fire spreading to other train carriages. However, in the actual environment of heavy railroad tunnels, there is typically a certain wind speed. After simulating the fire under a wind speed of 1 m/s, the surface temperature of the coal layer in the train carriages is illustrated in Figure 6.

As shown in Figure 6, the temperature in the compartment where the fire occurred is significantly higher and exhibits a fluctuating pattern. This is primarily due to the cooling effect of wind speed on the high-temperature smoke generated by the fire, while the local temperature on the surface of the transported coal exchanges heat with the high-temperature smoke produced by the fire, causing a temporary increase in local temperature. It can be clearly observed that at approximately 1067 s into the fire, the surface temperatures

of the adjacent compartments on both the upper and lower wind sides of the burning compartment are significantly above 300 °C, which has reached the basic combustion temperature of coal. Through numerical simulation software Pyrosim, it is evident that the fire spreads to the adjacent compartments, causing additional fires, as illustrated in the flame schematic in Figure 7.

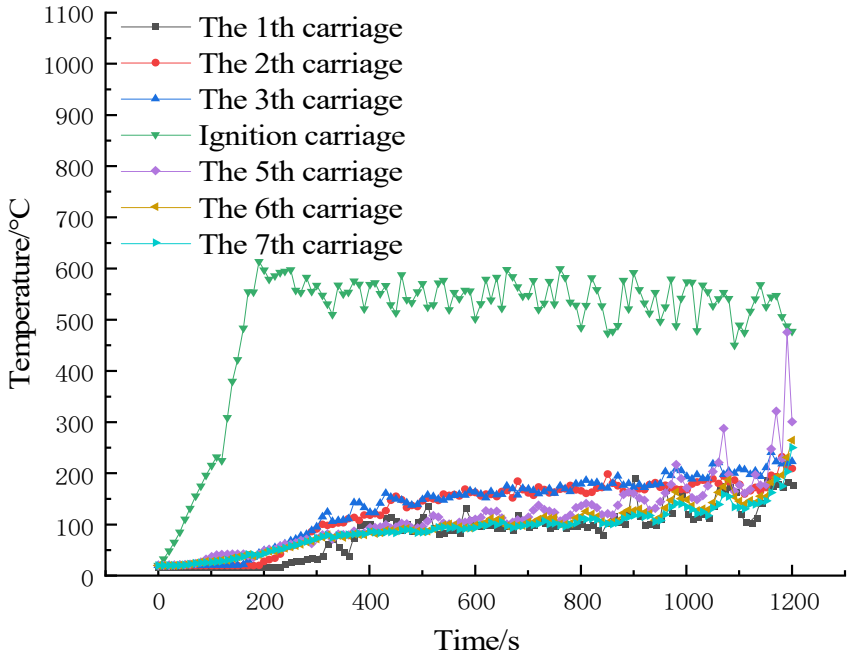


Figure 6. Temperature change diagram of the exposed surface of the coal seam in each carriage with a vertical height of 3.9 m.



Figure 7. Heavy railroad tunnel fire spread.

Figure 7 clearly indicates that the fire spreads not only to the downwind side of the ignition source but also to the upwind side. As the airflow moves towards the ignition source, it exerts a flexible damping effect on the high-temperature smoke being drawn in. This is primarily due to the increase in temperature near the ignition source, which causes a reduction in local air density on the upwind side of the ignition source. The hot smoke is buoyed upward, while the fresh airflow moving within the tunnel, consisting of air at normal temperature, creates a stratified flow with the high-temperature smoke near the ceiling, resulting in a reverse pressure gradient that suppresses normal air movement. Concurrently, this phenomenon allows the oxygen in the fresh airflow to be utilized more directly by the ignition source, thereby promoting the combustion process and significantly enhancing the heating effect, which may further strengthen the damping effect. As the high-temperature smoke moves towards the upwind side of the ignition source, it is also influenced by the fresh airflow, slowing down its movement and potentially settling locally near the ignition source for a certain period, thus facilitating heat accumulation. When coal is exposed to a high-temperature environment under these conditions for a certain duration, it will ignite. Therefore, this can lead to multi-source fires. The temperature cloud at the height of the compartment at 1067 s is illustrated in Figure 8.

Figure 8 clearly shows that the temperature of the carriage section is higher than that under windless conditions. Additionally, the temperature near the fire source in the

carriage is elevated, exceeding 300 °C, which is the ignition point of coal. This increase in temperature contributed to the spread of the fire.

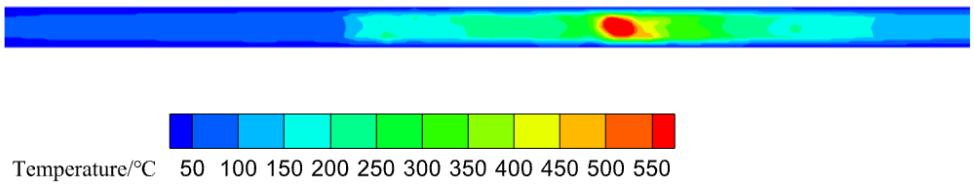


Figure 8. Vertical compartment height temperature cloud map.

Under specific ventilation conditions, although it is possible to control the local temperature decrease in a short period, the oxygen present in the ventilated environment will facilitate the combustion of the fire source, accelerating the rate of heat release from the fire. This not only leads to a rapid increase in fire temperature after a certain period but also causes the fire to spread to other compartments. Meanwhile, the high-temperature smoke that is drawn in will cause the average temperature of the entire tunnel to rise rapidly. This situation severely impacts personnel safety during evacuation and complicates rescue efforts. Additionally, excessive temperatures can inflict damage to the tunnel structure. Therefore, it is essential to determine the critical wind speed for fires in heavy railroad tunnels. At the same time, utilizing wind speed and other measures to prevent the high temperatures from the fire from igniting other carriages is crucial in suppressing the occurrence of multiple fire sources.

3.2. Determination of Critical Wind Speed for Fire in Heavy Railroad Tunnel

The critical wind speed refers to the wind speed condition under which the high-temperature smoke generated by a tunnel fire does not reverse its flow. In this scenario, the critical wind speed is not only crucial for controlling the movement trajectory of the smoke flow and preventing the fire from spreading to the upwind side of the compartment, but it is also an important factor in determining the wind speed conditions.

In the study of critical wind speed, it can be calculated and predicted using mathematical empirical formulas, as demonstrated in Equation (6).

$$v_{cr} = k\left(\frac{gQH}{c_p \rho_0 AT}\right)^{1/3} \tag{6}$$

where v_{cr} is the critical wind speed, m/s; k is a variable constant, which is mainly affected by the location and size of the fire source, and can take the value of 1 in the numerical simulation; H is the height of the heavy railroad tunnel, m; A is the cross-section area, m^2; T is the temperature of the smoke stream, K. Under the condition of no wind, the temperature is about 550 °C. The specific heat capacity of air is approximately 1.3818 kJ/(kg·K), and the critical wind speed is calculated to be around 2.14 m/s. To verify this calculation, a numerical simulation study of fire conditions was conducted at wind speeds of 2.1 m/s, 2.14 m/s, 2.2 m/s, and 2.3 m/s. The study focused on the maximum heat release rate during the fire, as well as the corresponding temperature profiles, which are illustrated in Figure 9.

The temperature cloud in Figure 9 clearly shows that when the heat release rate of the fire source reaches its peak, the fire temperature field stabilizes. Figure 9a illustrates the temperature cloud at a wind speed of 2.1 m/s, where it is evident that the high-temperature smoke generated by the fire is still partially receding backward. However, this backward receding phenomenon completely disappears at a wind speed of 2.14 m/s. This value aligns with the calculated results, allowing us to determine that the critical wind speed for this condition is 2.14 m/s. Furthermore, an observation and analysis of the temperature

distribution indicates that wind speed influences both the temperature peak and the average temperature within the fire area of the railroad tunnel, revealing a negative correlation between wind speed and temperature peak.

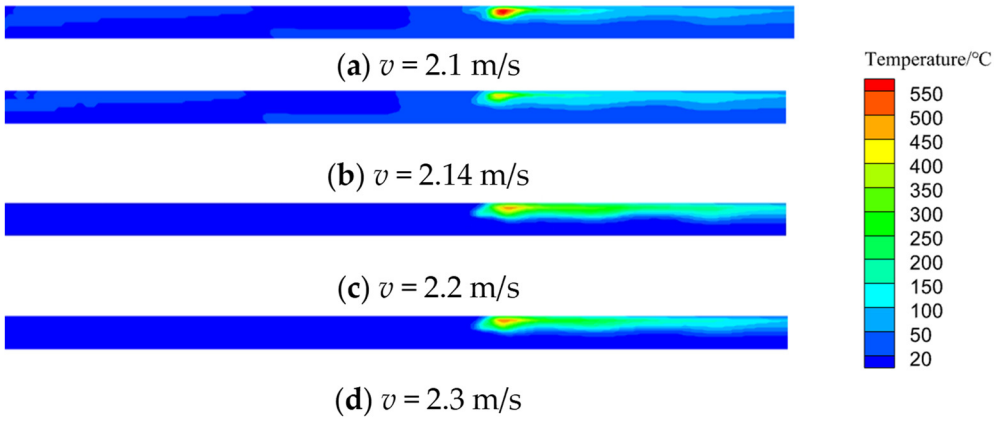


Figure 9. Temperature cloud for different wind speed conditions at 300 s.

3.3. Research on Flame Spread and Wind Speed Control of Fire in Heavy Railroad Tunnel

Different ventilation environments not only affect the temperature of tunnel fires but also lead to certain changes in flame shape. The flame shape is influenced by varying wind speeds, which can cause a certain deflection angle. Due to the special nature of the cargo transported by heavily loaded trains, excessively high wind speeds can increase the deflection angle of the flame. The thermal radiation from the flame can raise the surface temperature of coal on other unburned trains, potentially leading to fire outbreaks and creating multiple fire sources. Therefore, while ensuring that the wind speed in the tunnel is at the critical wind speed, it is also necessary to control the wind speed to prevent the spread of fire. The relationship between the flame deflection angle and wind speed can be calculated using Equation (7).

$$\theta = \arctan\left(\frac{v}{u_p}\right) \tag{7}$$

where v is the tunnel ambient wind speed, m/s; u_p is the flame vertical rise velocity, m/s. The flame vertical rise velocity can be described as Equation (8).

$$u_p = C\left(\frac{Q}{\rho_0 c_p T_0 D^2}\right)^{1/3} \tag{8}$$

where C is an empirical constant, taken as 1; D is the diameter of the fire source, m. After determining its deflection angle, its flame horizontal deflection distance x can be determined by Equation (9).

$$x = H \cdot \tan\left(\arctan\left(\frac{v}{u_p}\right)\right) \tag{9}$$

where H is the height of the flame, m. The distance between the front of the flame and the carriage transporting coal on the downwind side of the fire source can be calculated using Equation (10), which is shown below.

$$d = \sqrt{(L+x)^2 + H^2} \tag{10}$$

where d is the distance from the front of the flame to the coal compartment on the downwind side of the fire source, m. The heat radiation flux to which the coal on its downwind side is exposed can be calculated using Equation (11).

$$q'' = \varepsilon \sigma T_f^4 \cdot \frac{1}{4\pi d^2} \tag{11}$$

where, q'' is the thermal radiation flux kW/m^2; ε is the emissivity, take 0.9; σ is the Stefan–Boltzmann constant; T_f is the flame temperature, K.

Through calculations, it is determined that when the wind speed exceeds 2.3 m/s, the compartments on the downwind side of the fire source, located between 0.5 m and 3 m, have an increased likelihood of ignition. Numerical simulation software was employed to model the tunnel fire at a wind speed of 2.4 m/s. The results indicate that adjacent compartments on the downwind side of the fire begin to ignite at 719 s. Furthermore, by 825 s, the coal within these compartments is ignited, leading to the spread of the fire. The temperature distribution of the fire is illustrated in Figure 10.

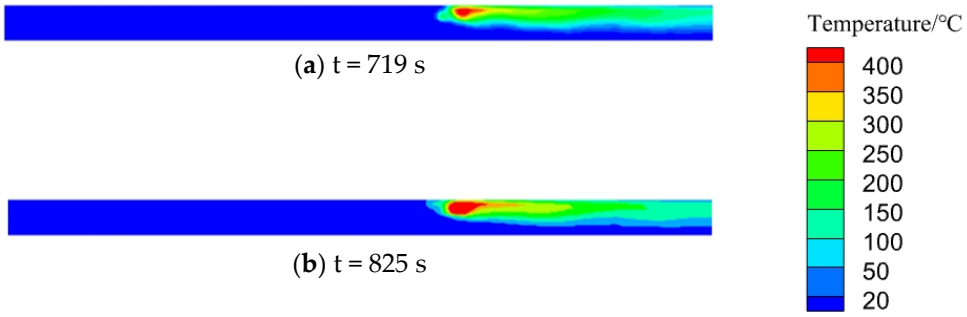


Figure 10. Fire temperature cloud at different moments when v = 2.4 m/s.

In Figure 10, panel (a) illustrates the downwind side of the carriage coal fire at the onset of the fire, where the temperature is relatively low. At this stage, the critical wind speed for the fire remains effective. However, as the heat release rate of the carriage coal gradually increases, the overall heat release rate of the fire rises, leading to the invalidation of the critical wind speed. This phenomenon is further evidenced in Figure 10b, where the high-temperature smoke exhibits the occurrence of inverse recession. This effect is primarily attributed to the increase in fire duration, which correlates positively with the heat release rate. It can be concluded that at 825 s into the fire, the combustion of coal produces an open flame. As the duration of the fire increases, the potential for its spread also rises. The heightened heat release rate exacerbates the smoke countercurrent phenomenon, which may facilitate the fire's spread to the upwind side. Concurrently, factors such as wind speed and thermal resistance may contribute to the fire spreading downwind. Therefore, it is essential to control wind speed and implement additional emergency measures. Currently, the primary fire prevention and suppression strategy in tunnels involves the use of water mist sprinklers. Water mist spraying effectively reduces the high temperatures generated by the fire and helps prevent its spread.

4. Study on the Effect of Water Mist Spraying on Temperature Distribution and Fire Spreading

4.1. Study of the Effect of Water Mist on the Temperature Field at Different Locations

The water mist spraying system not only reduces the temperature generated by a fire but also provides localized cooling to prevent the spread of flames. However, during actual fire scenarios, the thermal buoyancy produced by the fire can significantly affect the trajectory of the spray, preventing it from directly impacting the fire's surface [26–29]. Additionally, the high temperature of the fire plume can cause water mist with lower density to evaporate in such an environment, thereby diminishing its cooling effectiveness. Due to the high temperature of the fire plume, a low density of water mist can lead to evaporation in such an environment, thereby diminishing its cooling effect. Furthermore, wind speed significantly influences the trajectory of the water mist.

This study focuses on working conditions, specifically examining the critical wind speed conditions at the water spray location and the cooling effect of the impact. Additionally, it investigates the fire spread conditions associated with a wind speed of 2.4 m/s, particularly regarding combustible materials, to assess the effectiveness of water spray in preventing fire spread.

In analyzing the motion of water mist particles, their trajectory can be described using mechanistic formulas. Equation (12) represents the horizontal direction, while Equation (13) describes the trajectory in the vertical direction.

$$m_p \frac{du_{px}}{dt} = -\frac{1}{2} C_d \rho_0 A_p |v - u_{px}| (v - u_{px}) \tag{12}$$

$$m_p \frac{du_{py}}{dt} = -\frac{1}{2} C_d \rho_0 A_p |u_{py}| u_{py} - m_p g \tag{13}$$

where m_p is the mass of water mist particles, kg; u_{px} is the horizontal movement speed, m/s; u_{py} is the vertical movement speed, m/s; C_d is the coefficient of resistance, take 1; A_p is the projected area of the particles, m^2. Other water mist spray settings and conditions are shown in Table 2 [30].

Table 2. Water mist spray settings.

Water Mist Spray Related Conditions	Set of Parameters
Water discharge speed	14 m/s
Diameter of water mist particles	100×10^{-6} m
Water mist particle density	1000 kg/m^3
Initial horizontal speed	9.9 m/s
Initial vertical velocity	9.9 m/s
Spraying density	8 L/min·m^2

The path of water mist movement is influenced by wind speed. Under critical wind speed conditions, the mist tends to drift downwind from the fire source. Therefore, Equation (14) can be utilized to calculate its offset distance, as shown below.

$$L = vt \tag{14}$$

where L is the offset distance, m; t is the time for the water mist to fall to the upper surface of the carriage, s.

The calculations indicate that at a velocity of 2.14 m/s, the offset distance of the water mist is 4.1 m, while at a velocity of 2.4 m/s, the offset distance is approximately 4.8 m. Based on these calculations, it is essential to position the water mist sprinkler system on the upwind side of the fire, adjusting for varying wind speeds. This analysis compares the temperature cloud diagrams of a water mist sprinkler system located directly above the fire and one offset by 4.8 m on the upwind side, in contrast to a system without water mist. Figure 11 illustrates the temperature field comparisons before and after the fire occurred at 825 s, highlighting the effects of the water mist spraying system.

According to the research comparison presented in Figure 11, the cooling effect of water mist sprinklers set directly above the fire source is relatively significant, with the lowest temperature peak observed at a distance of 4.8 m from the fire source. This indicates that not only does the sprinkler system significantly suppress the heat release rate of the fire, but its effectiveness is also related to wind speed and the position of the water mist sprinklers. The off-centered sprinklers can directly impact the surface of the fire, while the water mist directly above the fire, although having some cooling effect, cannot directly act on the fire surface and only serves to lower the temperature. Compared to the absence of water mist, the temperature peak decreases less, with a local average temperature drop of

approximately 89 °C near the fire source. Under the conditions of the off-centered sprinkler operation, the suppression of the heat release rate results in a temperature reduction, maintaining temperatures below 300 °C at the height of the compartment. This suggests that the local temperatures in adjacent compartments, which did not experience a fire, did not reach the ignition point of coal, and the thermal radiation flux did not reach the critical thermal flux value necessary for coal combustion, leading to the cessation of fire spread. Additionally, the phenomenon of high-temperature smoke receding also disappears. Under wind speed conditions of 2.4 m/s, setting water mist sprinklers 4.8 m on the upwind side of the fire can effectively reduce the average temperature of the fire tunnel, with a temperature peak decrease of approximately 190 °C and an average temperature drop of about 140 °C, thereby suppressing the spread of the fire. At critical wind speed conditions, the likelihood of the fire spreading to other trains is low; therefore, the study primarily focuses on the impact of the optimized off-centered water mist sprinkler conditions on the escape environment at a height of 1.6 m, particularly under wind speed conditions of 2.4 m/s.

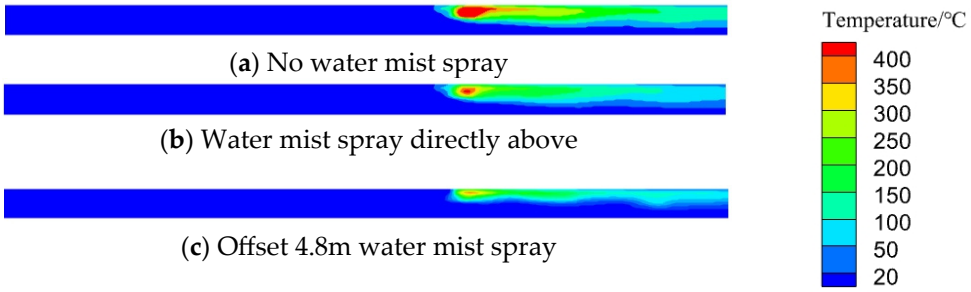


Figure 11. Temperature field comparison of 825 s with and without water mist spray system.

4.2. Study of the Effect of Water Mist Spray Conditions on the Environment for the Escape of People

When the wind speed reaches the critical threshold of 2.14 m/s, the vertical height on the downwind side of the fire corresponds to the characteristic height of the human eye. This parameter is essential for studying the temperature variations across different local areas, as illustrated in the temperature change trend graph shown in Figure 12.

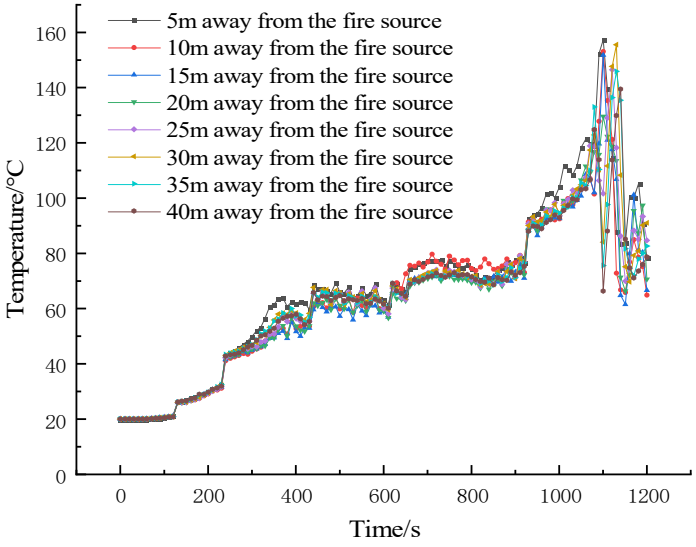


Figure 12. Trend chart of the temperature change of the personnel escape environment at the height of the human eye and the vertical height of 1.6 m.

At the time of the fire, the temperature at a vertical height of 1.6 m on both sides of the compartment was essentially uniform. As illustrated in Figure 12, the temperature change on the left side of the compartment indicates that approximately 430 s after the fire ignited, the local temperature exceeded 60 °C. This poses a significant threat to personnel attempting to escape. Subsequently, the temperature exhibited an upward trend, primarily due to its proximity to the high-temperature smoke layer. The primary reason for the temperature variation with vertical height is its predominant interaction with the high-temperature smoke layer for heat exchange and warming. Given that both ends of the tunnel serve as open exits, the accumulation of the smoke layer remains relatively shallow. Furthermore, the movement of airflow can lead to gradual temperature changes, whether increasing or decreasing, resulting in a slow upward trend in temperature.

The temperatures of each region in the 400 s, both with and without the application of water mist spray, were compared. The resulting comparison graph is presented in Figure 13.

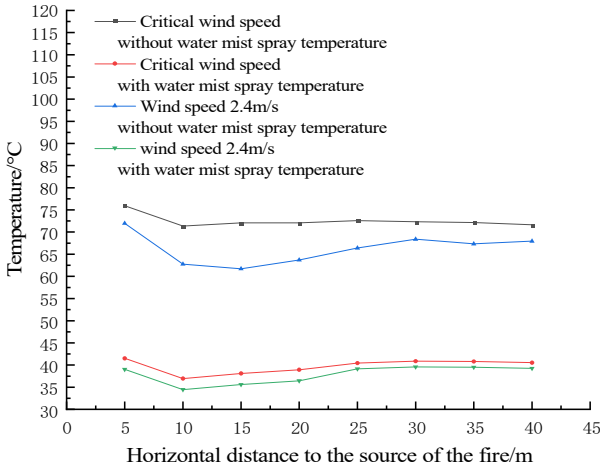


Figure 13. Cooling effect of water mist spraying at vertical height 1.6 m with different wind speeds at 400 s.

Figure 13 illustrates that by optimizing the offset amount of the water spray location, the cooling effect is significantly enhanced. This optimization aligns with personnel escape endurance conditions, thereby providing improved environmental conditions for firefighting and rescue operations.

5. Conclusions

(1) A numerical simulation of a 10 MW heavy railroad tunnel fire, with a peak temperature of 550 °C, was conducted. The results indicated that under ventilation conditions below the critical wind speed, smoke exhibited backward recession. Additionally, the fire spread to both the downwind and upwind sides, igniting adjacent compartments and resulting in multiple fire sources.

(2) This study employs theoretical analysis and numerical simulations to determine a critical wind speed of 2.14 m/s. Various wind speed conditions are simulated to explore the relationship between fire deflection angle and wind speed, as well as the heat radiation flux from the flame front on the downwind side of an adjacent train. Additionally, based on the combustion characteristics of coal, it is deduced that when the wind speed exceeds 2.4 m/s, the heat radiation flux on the surface of the fire source, located 0.5 m to 3 m downwind of the train, is sufficient to ignite the coal. The numerical simulations indicate that a fire event occurs at 719 s, leading to the ignition of coal in the neighboring compartments on the downwind side. This results

in significant burning in these compartments, with high-temperature smoke backing up to the boundary of the upwind side of the fire source by 825 s, ultimately leading to the failure of the critical wind speed.

(3) This study investigates the relationship between the water mist trajectory and wind speed. The trajectory of the water mist was analyzed under both horizontal and vertical initial speeds of 9.9 m/s. It was found that the water mist offset was 4.1 m at the critical wind speed and 4.8 m at a wind speed of 2.4 m/s. Furthermore, the offset was optimized from the initial position of the water mist spray, resulting in a significant cooling effect. Specifically, the peak temperature on the downwind side of the fire source was reduced from 77 °C to 42 °C at a height of 1.6 m, 400 s after the initiation of the spray. At this height, under critical wind speed conditions, the peak temperature on the downwind side of the fire source decreased from 77 °C to 42 °C after 400 s, while at a wind speed of 2.4 m/s, the peak temperature was reduced from 71 °C to 39 °C. The ambient temperature at a height of 1.6 m aligns with the endurance temperature necessary for personnel escaping from the optimized water mist spraying conditions.

(4) The unique characteristics of heavy railroad tunnel fires, along with the specific nature of train cargo transport, facilitate the rapid spread of fire. Low wind speeds can cause high-temperature smoke to reflux, consequently igniting combustion on the upwind side of the carriage. Furthermore, the peak temperature within the tunnel is significantly high, and there exists a negative correlation between wind speed and temperature peaks. Conversely, excessively high wind speeds can lead to an increased angle of flame deflection, which may ignite adjacent combustible materials downwind. The implementation of water spray systems can effectively mitigate fire spread and lower average temperatures, thereby aiding in the evacuation of individuals and enhancing emergency rescue efforts.

6. Discussion

This study investigates the fire characteristics during coal transportation in a heavy-load railway tunnel located in Shanxi Province. In theory, a fire occurring on a train during transport should be quickly detected, and personnel should evacuate promptly. However, the unique properties of coal make it challenging to identify a fire in its early stages without keen inspection. Generally, a freight train with a load of 20,000 to 30,000 tons requires at least 5 min of braking time. During this period, the train's movement continues to supply ample oxygen for coal combustion, potentially accelerating the fire. Therefore, based on the findings of this study, multiple sprinkler systems should be installed in the tunnel in advance, tailored to the properties of different cargo. Additionally, the locations of these sprinkler systems should be marked to indicate optimal stopping points for burning trains and ignition materials, ensuring that the water mist can function effectively. Real-time monitoring of the tunnel's wind speed is also essential; when the wind speed is too low, ventilation equipment should be used to supplement airflow, preventing the backflow of fire smoke within the tunnel and mitigating the risk of secondary disasters.

Author Contributions: W.H. was in charge of the ideas, formulae derivation. He also conducted the first draft of the paper, writing, and theoretical validation; M.F. and L.X. were responsible for the numerical simulation and theoretical analysis; M.F., S.Z. and W.H. were responsible for the numerical simulation and the experimental accuracy validation of the downscaled model; W.H. was responsible for the data visualization component; M.F., L.X. and W.H. were responsible for the collation of articles and correction of errors. All authors have read and agreed to the published version of the manuscript.

Funding: This study was supported by Guangdong Provincial University Innovation Team Project: Technology Innovation Team for Intelligent Application and Maintenance of Urban Rail Transit Equipment (2024KCXTD084); Characteristic Innovation Project of Colleges and Universities in Guangdong Province: Research on Quantitative Evaluation of Urban Rail Transit Safety Risk and Its Maintenance Strategy in the Guangdong-Hong Kong-Macao Greater Bay Area (2024KTSCX382); Guangzhou Philosophy and Social Science Planning Project: Yangcheng Green Beauty Travel Guide: Research on Accessibility Analysis and Path Optimization of "Blue Road Must Arrive" (2024GZGJ120); 2020 Excellent Online Course-Urban Rail Vehicle Structure Overhaul and Maintenance (ZC-AB-05-07-235K).

Data Availability Statement: Data and other information can be obtained by contacting e-mail address gd3987@outlook.com.

Conflicts of Interest: Author Shiqi Zheng was employed by the company Guangzhou Municipal Engineering Design & Research Institute Co., Ltd. The remaining authors declare that the research was conducted in the absence of any commercial or financial relationships that could be construed as a potential conflict of interest.

References

1. Zhao, S.; Liu, F.; Wang, F.; Weng, M. Experimental studies on fire-induced temperature distribution below ceiling in a longitudinal ventilated metro tunnel. *Tunn. Undergr. Space Technol.* **2018**, *72*, 281–293. [CrossRef]
2. Ji, J.; Wan, H.; Gao, Z.; Fu, Y.; Sun, J.; Zhang, Y.; Li, K.; Hostikka, S. Experimental study on flame merging behaviors from two pool fires along the longitudinal centerline of model tunnel with natural ventilation. *Combust. Flame* **2016**, *173*, 307–318. [CrossRef]
3. Liang, K.; Hao, X.F.; An, W.G.; Tang, Y.; Cong, Y. Study on cable fire spread and smoke temperature distribution in T-shaped utility tunnel. *Case Stud. Therm. Eng.* **2019**, *14*, 100433. [CrossRef]
4. Song, Y.J. Research on Key Risk Factors Identification and Control Strategies for Coal Railway Transportation in China. Master's Thesis, North China Electric Power University, Beijing, China, 2024.
5. Zhang, J.R.; Yang, J.F. Environmental impact analysis of coal transportation in Daqin Railway. In Proceedings of the 2020 Annual Conference of the Chinese Society for Environmental Sciences, Yuncheng, China, 18–21 October 2020; Volume 3, pp. 125–129.
6. Chen, C.J. The factors of affecting the effectiveness of coal quality inspection and countermeasures. *Coal Process. Compr. Utilization.* **2025**, *4*, 113–115.
7. Zhong, M.H.; Liu, C.; Yang, Y.X. Study on ventilation mode for train fire in metro tunnel with single-side slope. *J. Saf. Sci. Technol.* **2018**, *14*, 5–13.
8. Jae, S.R.; Seung, S.Y.; Hong, S.R.; Yoon, M.O.; Jeong, Y.T. An experimental study on the effect of ventilation velocity on burning rate in tunnel fire-heptane pool fire case. *Build. Environ.* **2008**, *43*, 1225–1231.
9. Chiara, V.; Bruno, F.; Emilio, P.; Maschio, G. Experimental study on thermal and toxic hazards connected to fire scenarios in road tunnels. *J. Loss Prev. Process Ind.* **2012**, *25*, 718–729.
10. McGrattan, K.; Hamins, A. *Numerical Simulation of the Howard Street Tunnel Fire*; NISTIR6902; National Institute of Standards and Technology: Gaithersburg, MD, USA, 2002.
11. Ciro, C.; Paolo, C. Simulation of fire scenarios due to different vehicle types with and without traffic in a bi-directional road tunnel. *Tunn. Undergr. Space Technol.* **2013**, *37*, 22–36.
12. Jia, Y.; Fan, X.L.; Zhao, X.J.; Deng, Y.L.; Zhu, X.L.; Zhao, W.F. Study on the longitudinal ceiling temperature distribution induced by double pool fires in a tunnel. *Int. J. Therm. Sci.* **2021**, *168*, 107059. [CrossRef]
13. Wang, Q.; Wang, S.; Liu, H.; Shen, J.; Shang, F.; Shi, C.; Tang, F. Characterization of ceiling smoke temperature profile and maximum temperature rise induced by double fires in a natural ventilation tunnel. *Tunn. Undergr. Space Technol. Inc. Trenchless Technol. Res.* **2020**, *96*, 103233. [CrossRef]
14. Li, Y.X. Coal Spontaneous Combustion Characteristics in Low-temperature Oxidation Environment and Anti Spontaneous Combustion Countermeasures for Railway Coal Transportation. *Railw. Logist.* **2024**, *42*, 24–30.
15. Delichatsios, M. Flow of fire gases under a beamed ceiling. *Combust. Flame* **1981**, *43*, 1–10. [CrossRef]
16. Thomas, P.H. The movement of buoyant fluid against a stream and the venting of under ground fires. *Fire Saf. Sci.* **1958**, *351*, 1.
17. Thomas, P.H. *The Movement of Smoke in Horizontal Passages Against Air Flow*; Fire Research Technical Paper; Fire Research Station: Borehamwood, UK, 1968; Volume 7, pp. 1–8.
18. Hu, L.H.; Huo, R.; Chow, W.K. Studies on buoyancy-driven back-layering flow in tunnel fires. *Exp. Therm. Fluid Sci.* **2008**, *32*, 1468–1483. [CrossRef]

19. Yang, D.; Hu, L.H.; Huo, R.; Jiang, Y. Effects of Longitudinal Air Flow on Smoke Stratification in Channel Fire. *J. Combust. Sci. Technol.* **2010**, *16*, 5.
20. Wu, Y.; Bakar, M.Z.A. Control of smoke flow in tunnel fires using longitudinal ventilation systems-a study of the critical velocity. *Fire Saf. J.* **2000**, *35*, 363–390. [CrossRef]
21. Wang, C.; Guo, D.; Xu, B.; Liu, C.; Miao, Z. Experimental and numerical simulation study on fire spreading of urban cable tunnels. *J. Tsinghua Univ. (Sci. Technol.)* **2025**, *65*, 532–546.
22. Zhao, X.; Ni, M.; Wang, W.; Wang, H.; Wang, J. Study on the Fire Characteristics of Dual Fire Sources and the Difference in Power Temperature of Different Fire Sources in Tunnel. *Fire* **2024**, *7*, 273. [CrossRef]
23. Sumic, D.; Males, L.; Rosic, M. An Agent-Based Ship Firefighting Model. *J. Mar. Sci. Eng.* **2021**, *9*, 902. [CrossRef]
24. International Union of Railways. *UIC 564-2: Passenger Rolling Stock—Protection Measures Against Fire and Panic—Part 2: Design Requirements*, 3rd ed.; Union Internationale des Chemins de fer (UIC): Paris, France, 2019.
25. Qin, R.; Li, X.J. Study on the Grid Selection of Block Scale Pyrosim Fire Simulation. *Urban. Archit.* **2021**, *18*, 107–109.
26. Enrico, R. Testing the predictive capabilities of evacuation models for tunnel fire safety analysis. *Saf. Sci.* **2013**, *59*, 141–153.
27. Liu, Y.; Wang, Z.; Zhu, S.; Sun, L.; Wei, Q.; Zhou, X.; Cui, Y.; Wu, D. Research on the Infrared Cooling Characteristics of Composite Nozzle with Water Mist and Water Curtain. *J. Mech. Eng.* **2024**, *60*, 320–328.
28. Kalech, B.; Bouterra, M.; Elcafsi, A. Numerical analysis of smoke flow under the effect of longitudinal airflow in a tunnel fire. *Fire Mater.* **2020**, *44*, 1033–1043. [CrossRef]
29. Rickard, H. Fire behavior of multiple fires in a mine drift with longitudinal ventilation. *Int. J. Min. Sci. Technol.* **2019**, *29*, 245–254.
30. Tian, L. Research on the Evolution Law of Mine Belt Fire and the Prevention and Extinguishing Technology of Fine Water Mist. Master's Thesis, Hunan University of Science and Technology, Xiangtan, China, 2022.

Disclaimer/Publisher's Note: The statements, opinions and data contained in all publications are solely those of the individual author(s) and contributor(s) and not of MDPI and/or the editor(s). MDPI and/or the editor(s) disclaim responsibility for any injury to people or property resulting from any ideas, methods, instructions or products referred to in the content.